

## Investigation of Diffusion Kinetics of Borided X6Cr17 Steel

İsmail Yıldız\*

*Department of Machine Education, Iscehisar Vocational Schools,  
Afyon Kocatepe University, Afyonkarahisar, Turkey*

İbrahim Güneş

*Department of Metallurgical and Materials Engineering,  
Faculty of Technology, Afyon Kocatepe University, Afyonkarahisar, Turkey*

### ABSTRACT

In this study, the case properties and diffusion kinetics of DIN X6Cr17 steel borided in Ekabor-II powder were investigated by conducting a series of experiments at temperatures of 1123, 1223 and 1323K for 2, 4 and 6 h. The boride layer was characterized by optical microscopy, X-ray diffraction technique and micro-Vickers hardness tester. X-ray diffraction analysis of boride layers on the surface of the steels revealed the existence of  $Fe_xB_y$ ,  $Cr_xB_y$  and  $Ni_xB_y$  compounds. The thickness of boride layer increases by increasing boriding time and temperature for all steels. Depending on the chemical composition of substrates, the boride layer thickness on the surface of the X6Cr17 steel was found to be 50.48  $\mu\text{m}$  and 91.62  $\mu\text{m}$ , respectively. The hardness of the boride compounds formed on the surface of the X6Cr17 steel ranged from 1658 to 2284  $HV_{0.1}$ .

**Keywords:** X6Cr17, Boride layer, Micro-hardness, Kinetics, Activation energy

### 1 INTRODUCTION

Boronizing is a thermochemical treatment in which boron atoms are diffused into the surface of a workpiece and form borides with the base metal. The treatment has been applied to a wide range of materials including ferrous materials, non-ferrous materials and some super alloys [1-4].

Diffusion of boron into the surface of metals and alloys forms metallic borides, such as FeB and  $Fe_2B$ , depending on process temperature, chemical composition of substrate materials, boron potential of the medium and boriding time [5-7]. The process temperature is in the range of 700–1000 °C [8-10].

Once boron is deposited on the surface, the diffusion rate of boron through the matrix is controlled by the process temperature and time [11-13]. In general, the diffusion rate of boron is higher at higher temperatures, while time is critical for the thickness and composition of the boride layer. Additionally, the chemical composition of the substrate material is another important parameter and plays a major role in boron diffusion [14]. The hardness of boride layers is typically in the range of 1400–2100 HV and the thicknesses up to 380  $\mu\text{m}$  may be formed depending on the process time and temperature and on the alloying elements present in the substrate [15-17].

The main objective of this study was to investigate the rate of growth of boride layers on X6Cr17 steel and the effect of process parameters, such as temperature, time and chemical composition, on the

boride layers formed on the DIN X6Cr17 steel after powder pack boriding at different processing temperatures and times.

## 2 EXPERIMENTAL DETAILS

### 2.1 Boriding and Characterization

Table 1 presents the composition of the untreated DIN X6Cr17 steel.

Table 1 The chemical composition of test materials (wt.%)

Steels	C	Si	Mn	Cr	Ni
DIN X6Cr17	0.12	0.90	0.70	16.5	-

The test specimens were cut into Ø25x8mm dimensions, ground up to 1000G and polished using diamond solution. The boriding heat treatment was carried out in a solid medium containing an Ekabor-II powder mixture placed in an electrical resistance furnace operated at the temperature of 1123K, 1223K and 1323K for 2, 4 and 6 h under atmospheric pressure. The microstructures of polished and etched cross-sections of the specimens were observed under a Nikon MA100 optical microscope. The presence of borides formed in the coating layer was confirmed by means of X-ray diffraction equipment (Shimadzu XRD 6000) using Cu K $\alpha$  radiation. The thickness of borides was measured by means of a digital thickness measuring instrument attached to an optical microscope (Nikon MA100). The hardness measurements of the boride layer on each steel and untreated steel substrate were made on the cross-sections using a Shimadzu HMV-2 Vickers indenter with a 100 g load.

### 2.2 Evaluation of the activation energy of the boron diffusion

In order to study the diffusion mechanism, borided X6Cr17 steel was used for this purpose. It is assumed that the boride layers grow parabolically in the direction of diffusion flux and perpendicular to the substrate surface. So, the time dependence of boride layer thickness can be described by Eq. (1):

$$x^2 = Dt \quad (1)$$

where  $x$  is the depth of the boride layer (mm),  $t$  the boriding time (s),  $D$  the boron diffusion coefficient through the boride layer. It is a well-known fact that the main factor limiting the growth of a layer is the diffusion of boron into the substrate. It is possible to argue that the relationship between growth rate constant,  $D$ , activation energy,  $Q$ , and the temperature in Kelvin,  $T$ , can be expressed as an Arrhenius equation (Eq. (2)):

$$D = D_0 \exp\left(-\frac{Q}{RT}\right) \quad (2)$$

where  $D_0$  is a pre-exponential constant,  $Q$  the activation energy (J/mol),  $T$  the absolute temperature in Kelvin and  $R$  is the ideal gas constant (J/mol K).

The activation energy for the boron diffusion in the boride layer is determined by the slope obtained in the plot of  $\ln D$  vs.  $\frac{1}{T}$ , using Eq. (3):

$$\ln D = \ln D_0 - \frac{Q}{RT} \quad (3)$$

### 3 RESULTS AND DISCUSSION

#### 3.1 Characterization of boride coatings

The cross-section of the optical micrographs of the borided X6Cr17 steels at the temperature of 1123K and 1323K for 2 and 6 h are shown in Figures 1.

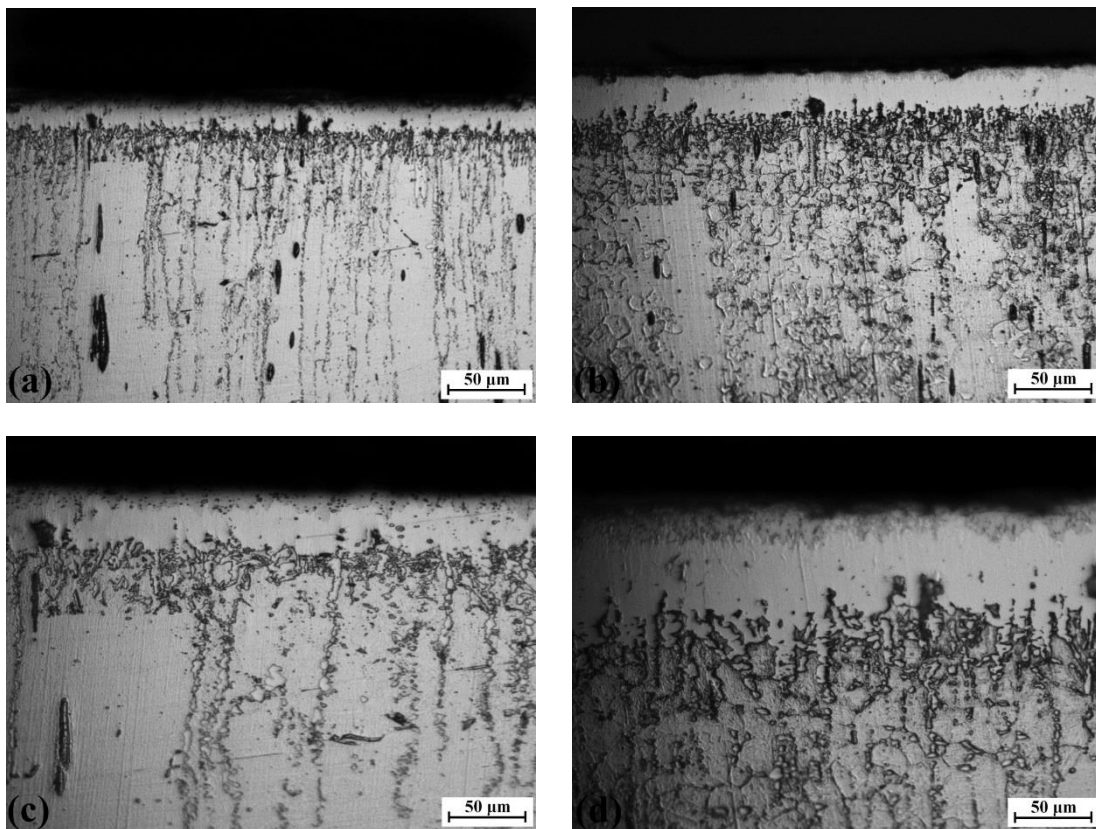


Figure 1: The cross-section of borided DIN X6Cr17 steel; a) 1123K - 2h, b) 1123K - 6h, c) 1323K - 2h, d) 1323K - 6h.

As can be seen the borides formed on the DIN X6Cr17 steel have a smooth and regular morphology. It was found that the coating/matrix interface and matrix could be significantly distinguished and the boride layer had a not columnar structure. Depending on the chemical composition of substrates, the boride layer thickness on the surface of the X6Cr17 steel was found to be 50.48  $\mu\text{m}$  and 91.62  $\mu\text{m}$ , respectively in Figures 2.

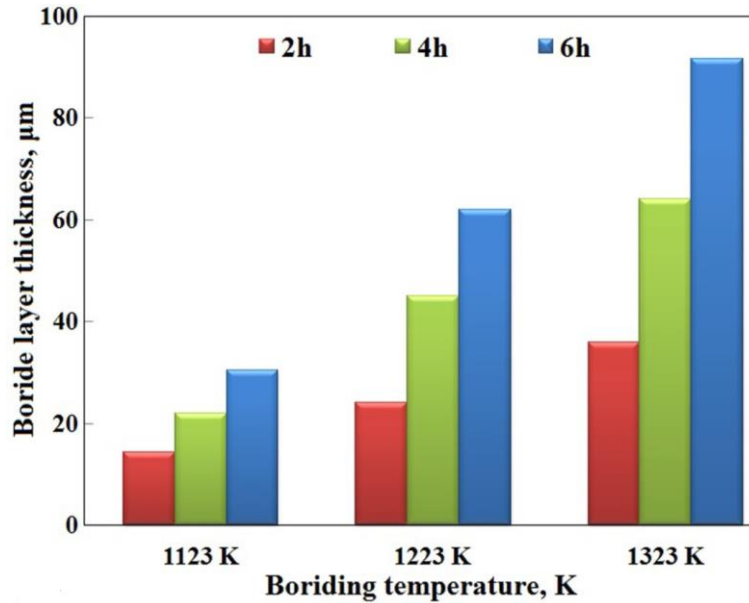


Figure 2: The thickness values of boride layers with respect to boriding time and temperatures

Figure 3 gives the XRD pattern obtained at the surface of borided DIN X6Cr17 steel at 1123K and 1323K for treatment time 2 and 6 h.

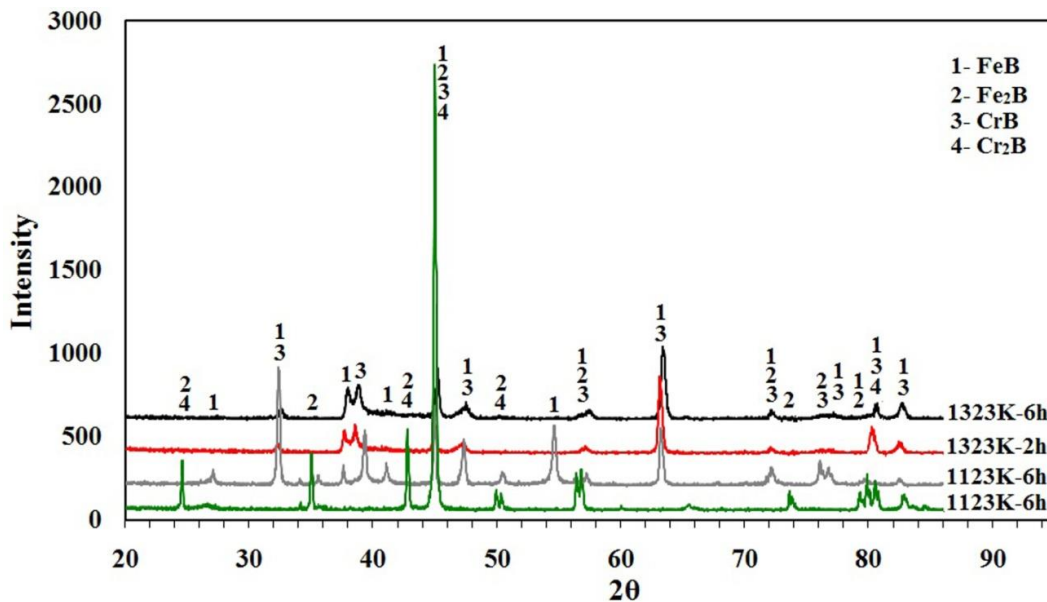


Figure 3: X-ray diffraction patterns of borided steel

XRD patterns show that the boride layer consists of borides such as MB and M<sub>2</sub>B (M=Metal; Fe, Cr, Ni). XRD results showed that boride layers formed on the DIN X6Cr17 stainless steels contained FeB, Fe<sub>2</sub>B, CrB, Cr<sub>2</sub>B phases, respectively (Figs. 3). The boride layers mainly consist of double intermetallic

phase (FeB and Fe<sub>2</sub>B) as a result of diffusion of boron atoms from boriding compound to metallic lattice with respect to the holding time.

Micro-hardness measurements were carried out from the surface to the interior along a line in order to see the variations in the boride layer hardness, transition zone and matrix, respectively. Micro-hardness of the boride layers was measured at 10 different locations at the same distance from the surface and the average value was taken as the hardness. Micro-hardness measurements were carried out on the cross-sections from the surface to the interior along a line; see Figs. 4. The hardness of the boride layer formed on the surface of the DIN X6Cr17 steel ranged from 1762 to 2165 HV<sub>0.1</sub> respectively, whereas Vickers hardness values of the untreated steel DIN X6Cr17 was 276 HV<sub>0.1</sub> and 328 HV<sub>0.1</sub>, respectively. When the hardness of the boride layer is compared with the matrix, boride layer hardness is approximately eight times greater than that of the matrix.

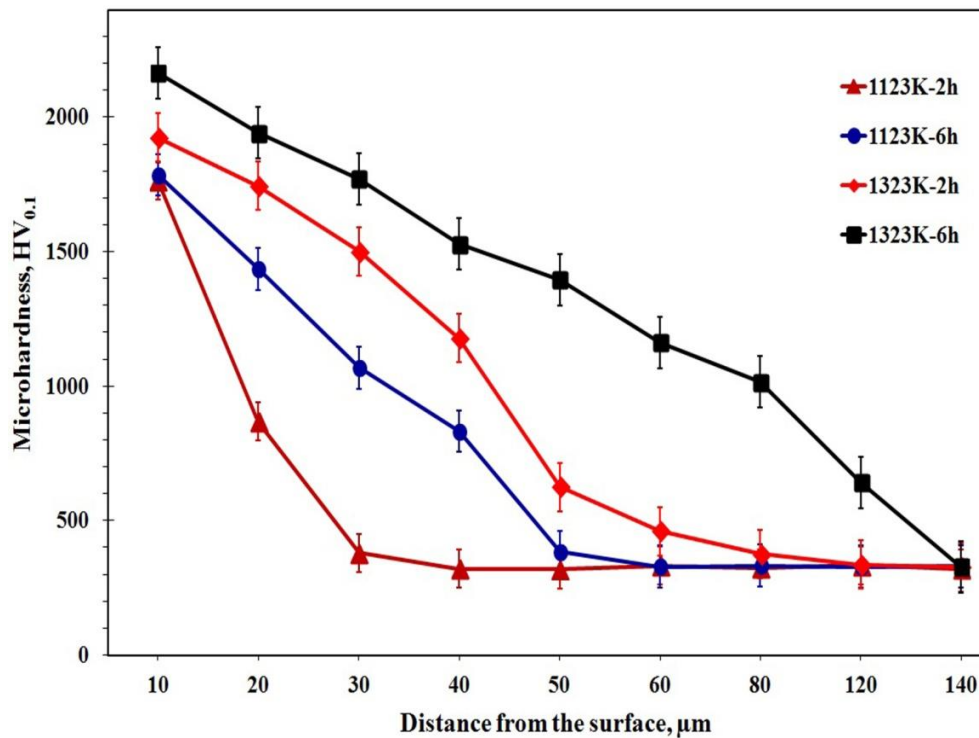


Figure 4: The variation of hardness depth in the borided steel

### 3.2 Kinetics

In this study, the effects of the processing temperature and boriding time on the growth kinetics of the boride layer were also investigated. Kinetic parameters such as processing temperature and time must be known for the control of the boriding treatment. Figure 5 shows the time dependence of the squared value of boride layer thickness at increasing temperatures. This evolution followed a parabolic growth law where the diffusion of boron atoms is a thermally activated phenomenon. The growth rate constant  $D$  at each boriding temperature can be easily calculated from Eq. (1).

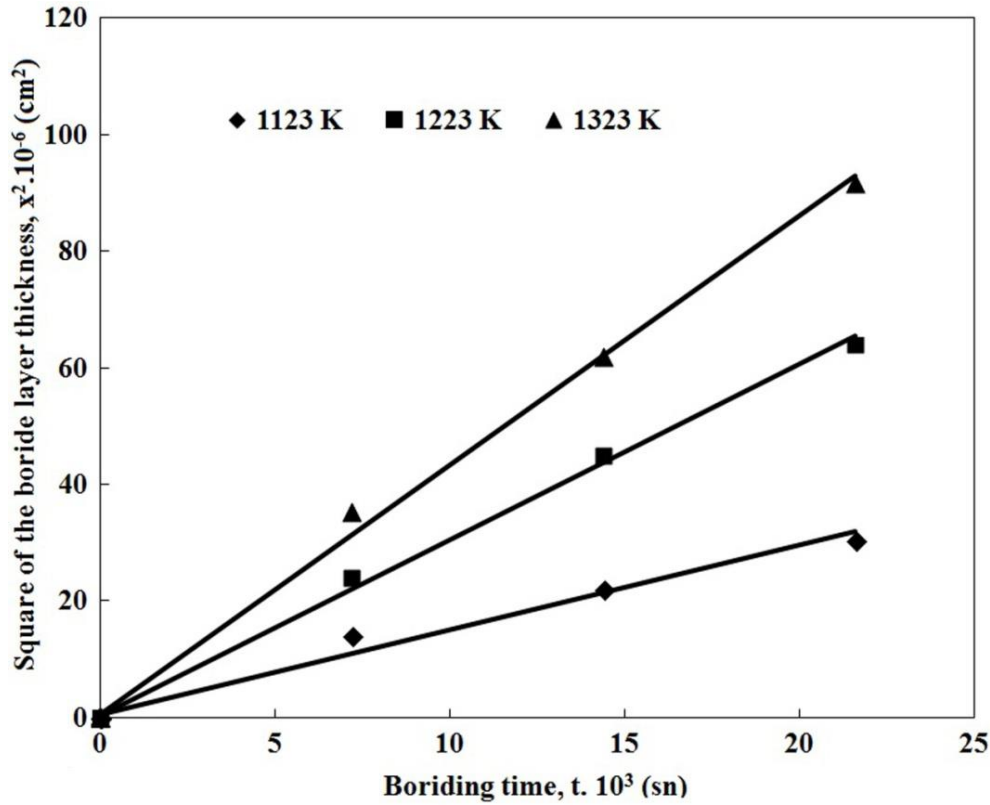


Figure 5: The time dependence of squared boride layer thickness at increasing temperatures

As a result, the calculated growth rate constants at the three temperatures: 1123, 1223 and 1323 K are the following:  $0.12 \times 10^{-9}$ ,  $0.40 \times 10^{-9}$  and  $1.89 \times 10^{-9} \text{ cm}^2 \text{ s}^{-1}$  for DIN X6Cr17 steel, respectively (Table 2).

Table 2 The growth rate constant (D) as a function of boriding temperature.

Material	Growth rate constant ( $\text{cm}^2 \text{ s}^{-1}$ )		
	Temperature, K		
	1123 K	1223 K	1323 K
DIN X6Cr17	$0.12 \times 10^{-9}$	$0.40 \times 10^{-9}$	$1.89 \times 10^{-9}$

Figure 6 describes the temperature dependence of the growth rate constant. The plot of  $\ln D$  as a function of the reciprocal temperature exhibits a linear relationship according to the Arrhenius equation. The boron activation energy can be easily obtained from the slope of the straight line presented on Figures 6. The value of boron activation energy was then determined as equal to 134.95 kJ/mol for DIN X6Cr17 steel.

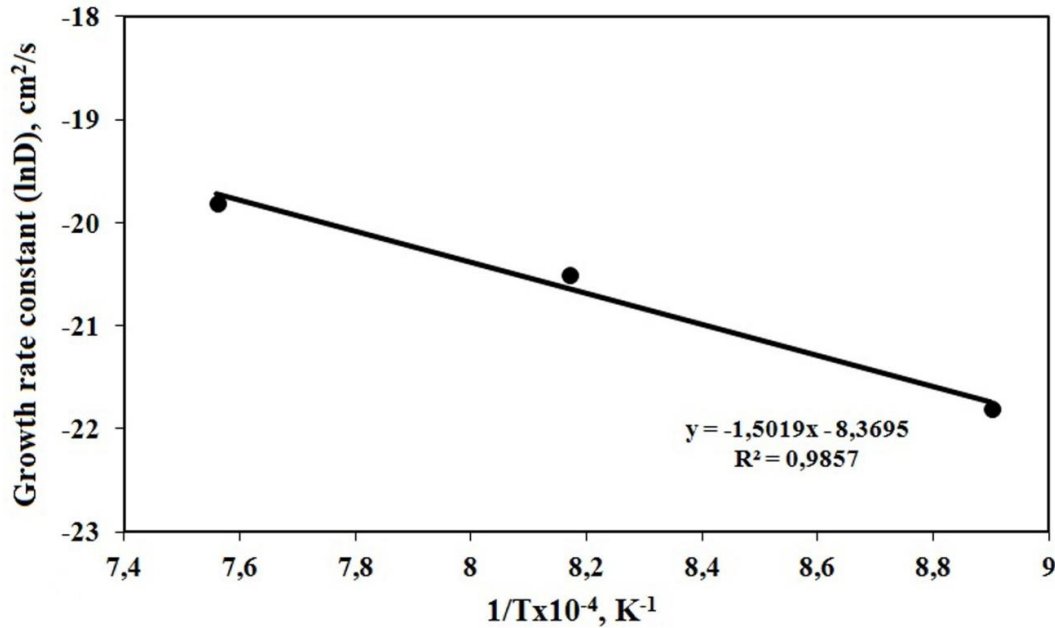


Figure 6: The temperature dependence of the growth rate constant according to the Arrhenius equation

Table 3 compares the obtained values of energy with the data found in the literature. It is seen the reported values of boron activation energy depended on the chemical composition of the substrate and on the used boriding method. The calculated value in this study is compatible with the values reported in the literature as seen in Table 3 [18-20].

Table 3 The comparison of activation energy for diffusion of boron with respect to the different boriding medium and substrates

Steel	Temperature range (K)	Boriding medium	Activation energy (kJ/mol)	References
DIN 304	1073–1223	Salt bath	253.35	[18]
DIN 304	1023-1223	Plasma paste	123	[19]
DIN 316	1073–1223	Pack	199	[20]
DIN X6Cr17	1123-1323	Pack	165.45 134.95	Present study

A contour diagram describing the evolution of boride layer thickness as a function of the boriding parameters (time and temperature) is shown in Figure 7. This contour diagram can be used for two purposes: (1) to predict the coating layer thickness with respect to the process parameters, namely time and temperature; (2) to determine the value of process time and temperature for obtaining a predetermined coating layer thickness [17,20,21]. The boride layer increased with the increase in boriding time and temperature in the borided X6Cr17 stainless steel.

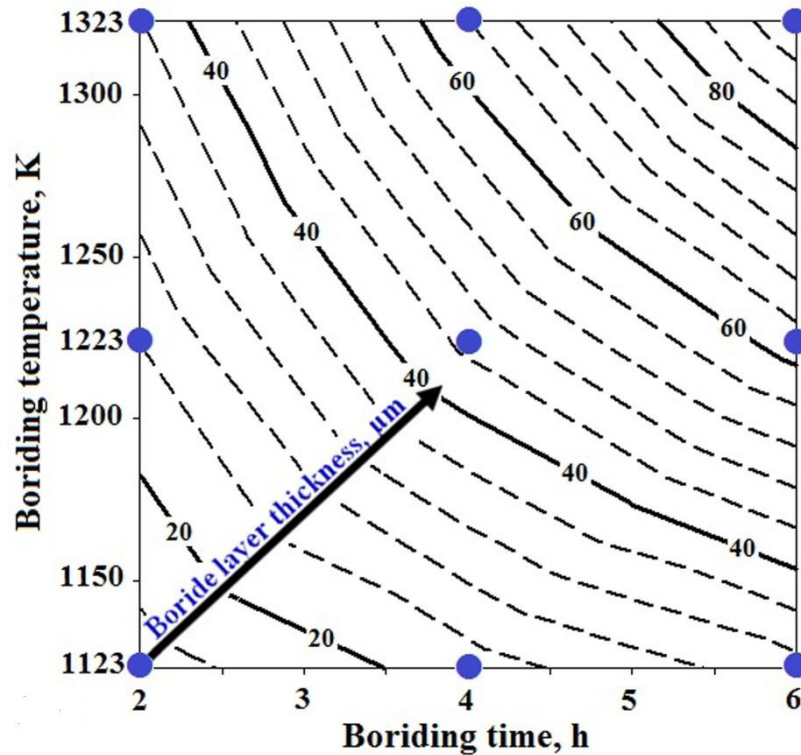


Figure 7: Contour diagram describing the evolution of boride layer thickness as a function of boriding parameters

#### 4 CONCLUSIONS

The following conclusions may be derived from the present study.

- Boride types formed on the surface of the stainless steels have smooth and regular structure.
- The boride layer thickness on the surface of the DIN X6Cr17 steel was obtained, depending on the chemical composition of substrates, 91.62  $\mu\text{m}$ , respectively
- The multiphase boride coatings that were thermo chemically grown on the DIN X6Cr17 steel was constituted by the FeB, Fe<sub>2</sub>B, CrB, Cr<sub>2</sub>B phases, respectively.
- The surface hardness of the borided DIN X6Cr17 steel was in the range of 1762-2165 HV<sub>0,1</sub>, while for the untreated DIN X6Cr17 steel substrate it was 328 HV<sub>0,1</sub>.
- Activation energy of 134.95 kJ/mol for DIN X6Cr17 steel was determined.

#### REFERENCES

- [1] Jain, V. and Sundararajan, G. (2002). Influence of the pack thickness of the boronizing mixture on the boriding of steel, *Surface & Coatings Technology*, 149, 21-26.
- [2] Kartal, G., Eryilmaz, O.L., Krumdick, G., Erdemir, A. and Timura, S. (2011). Kinetics of electrochemical boriding of low carbon steel, *Applied Surface Science*, 257, 6928–6934.



- [3] Campos-Silva, I., Ortiz-Domínguez, M., Bravo-Bárceñas, O., Doñu-Ruiz, M.A., Bravo-Bárceñas, D., Tapia-Quintero, C. and Jiménez-Reyes, M.Y. (2010). Formation and kinetics of FeB/Fe<sub>2</sub>B layers and diffusion zone at the surface of DIN 316 borided steels, *Surface & Coatings Technology*, 205, 403-412.
- [4] Xingliang H., Huaping X., Ozaydin, M. F., Balzuweit, K. and Liang, H. (2015). Low-temperature boriding of high-carbon steel, *Surface & Coatings Technology*, 263, 21-26.
- [5] Kayali., Y., Gunes, I. and Ulu, S. (2012). Diffusion kinetics of borided DIN 52100 and DIN 440C steels, *Vacuum*, 86, 1428-1434.
- [6] Genel, K. (2006). Boriding kinetics of H13 steel, *Vacuum*, 80, 451-457.
- [7] Sen, S., Sen, U. and Bindal, C. (2005). The growth kinetics of borides formed on boronized DIN 4140 Steel, *Vacuum*, 77, 195-202.
- [8] Kulka, M., Makuch, N., Pertek, A. and Piasecki, A. (2012). An alternative method of gas boriding applied to the formation of borocarbured layer, *Materials Characterization*, 72, 59-67.
- [9] Bataev, I. A., Bataev, A. A., Golkovsky, M. G., Teplykh, A. Y., Burov, V.G. and Veselov, S.V. (2012). Non-vacuum electron-beam boriding of low-carbon steel, *Surface & Coatings Technology*, 207, 245-253.
- [10] Oliveira, C. K. N., Casteletti, L. C., Lombardi Neto, A., Totten, G. E. and Heck, S. C. (2010). Production and Characterization of Boride Layers on DIN D2 Tool Steel, *Vacuum*, 84, 792-796.
- [11] Kartala, G., Eryilmaz, O.L., Krumdick, G., Erdemir, A. and Timura, S. (2011). Kinetics of electrochemical boriding of low carbon steel, *Applied Surface Science*, 257, 6928–6934.
- [12] Kulka, M., Makuch, N., Pertek, A. and Piasecki, A. (2012). Microstructure and properties of borocarbured and laser-modified 17CrNi6-6 steel, *Optics & Laser Technology*, 44, 872-881.
- [13] Makuch, N. and Kulka, M. (2014). Microstructural characterization and some mechanical properties of gas-borided Inconel 600-alloy, *Applied Surface Science*, 314, 1007-1018.
- [14] Taktak, S. (2007). Some mechanical properties of borided DIN H13 and 304 steels, *Materials and Design*, 28, 1836-1843.
- [15] Tabura, M., Izciler, M., Gul, F. and Karacan, I. (2009). Abrasive wear behavior of boronized DIN 8620 steel, *Wear*, 266, 1106-1112.

- [16] 16. Gunes, I. (2013). Wear Behaviour of Plasma Paste Boronized of DIN 8620 Steel with Borax and B<sub>2</sub>O<sub>3</sub> Paste Mixtures, *J. Mater. Sci. Technol.*, 29(7), 662-668.
- [17] Uslu, I., Comert, H., Ipek, M., Celebi, F.G., Ozdemir, O. and Bindal, C. (2007). A comparison of borides formed on DIN 1040 and DIN P20 steels, *Materials and Design*, 28,1819-1826.
- [18] Taktak, S. (2006). A study on the diffusion kinetics of borides on boronized Cr-based steels, *J. Mater. Sci.*, 41, 7590–7596.
- [19] Yoon, J. H., Jee, Y.K. and Lee, S.Y. (1999). Plasma paste boronizing treatment of the stainless steel DIN 304, *Surf. & Coat. Techn.*, 112, 71–75.
- [20] Ozdemir, O., Omar, M. A., Usta, M., Zeytin, S., Bindal, C. and Ucisik, A. H. (2009). An investigation on boriding kinetics of DIN 316 stainless steel, *Vacuum*, 83, 175-179.
- [21] Kahvecioglu, O., Sista, V., Eryilmaz, O.L., Erdemir, A. and Timur, S. (2011). Ultra-fast boriding of nickel aluminide, *Thin Solid Films*, 520, 1575-1581.